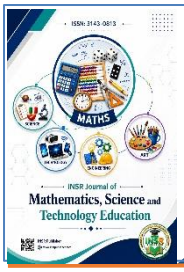

Open Access
Volume 02, Issue 08 - 2026

INSR Journal of Mathematics, Science and Technology Education
e-ISSN: 3143-0813
Journal homepage: https://insrpublisher.com/insrjmste/

Research Article

DOI: 10.5281/zenodo.22148593

On the formalism of the Lotka-Volterra equation and its application to melanoma growth

*** Matheus dos Santos Farias**
Postgraduate in nuclear physics with an emphasis on dynamical systems (Chaos Theory) USP.

Submission Date: 20 June 2026 **Published Date:** 28 August 2026

Citation: Farias, M. dos S. (2026). On the formalism of the Lotka-Volterra equation and its application to melanoma growth. In INSR Journal of Mathematics, Science and Technology Education (Vol. 2, Number 8, pp. 47–63). https://doi.org/10.5281/zenodo.22148593

Abstract

This work presents a formal mathematical derivation of the Lotka–Volterra system and its application to melanoma growth under fractionated radiotherapy. The model is derived from population balance, intrinsic growth or depletion assumptions, and bilinear interaction principles, leading step by step to the classical two-population Lotka–Volterra equations. After the analytical model is obtained, the radiotherapy component is introduced separately as an external dose input, preserving the two-dimensional population state space. The formulation is implemented numerically in C++ using a fourth-order Runge–Kutta scheme and coupled conceptually to a Geant4 Monte Carlo simulation of a clinically inspired treatment protocol. The study emphasizes the mathematical formalism and reproducible computational pathway rather than claiming patient-specific clinical validation.

Keywords: Lotka–Volterra system; melanoma; mathematical derivation; C++; Runge–Kutta method; Geant4; Monte Carlo simulation; radiotherapy; mathematical oncology.

Introduction

Huang et al. (2023) describe melanoma as a major global malignancy with substantial incidence and mortality, while Altrock et al. (2015) emphasize the role of mathematical oncology in representing tumor evolution through quantitative dynamical models. In this context, Lotka–Volterra-type formulations provide a compact nonlinear structure for studying interactions between modeled populations. The present study focuses not only on numerical simulation, but on the formal construction of the governing equations before computation. The mathematical model is first derived analytically, then translated into a numerical algorithm, and only afterward coupled to the radiotherapy dose used in the computational treatment scenario.

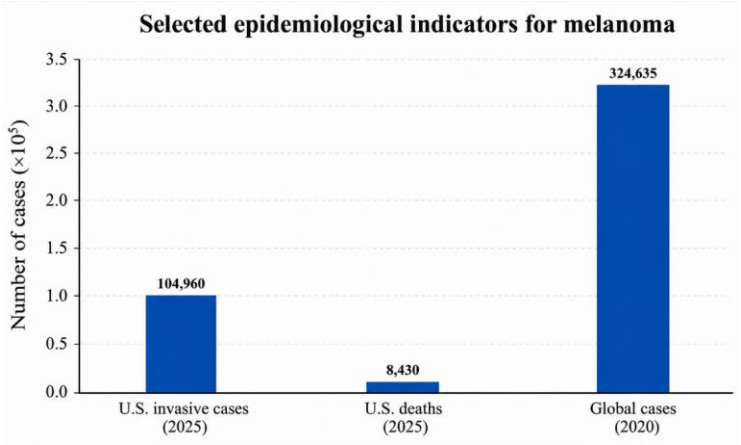

Figure 1: Lollipop-style epidemiological summary for melanoma, combining current U.S. estimates and recent global registry-based incidence data.

West et al. (2023) and Gallasch et al. (2013) show that computational cancer modeling commonly combines mathematical formulations with numerical simulation and treatment-response analysis. The present work adopts a complementary approach by making the analytical origin of the Lotka–Volterra equations explicit. Rather than introducing the final equation as a ready-made computational formula, the assumptions are stated, the individual contributions are constructed, and the limiting process leads to the final differential system. Once the Lotka–Volterra equations have been obtained, the radiotherapy variables are introduced as external treatment inputs rather than as additional Lotka–Volterra populations.

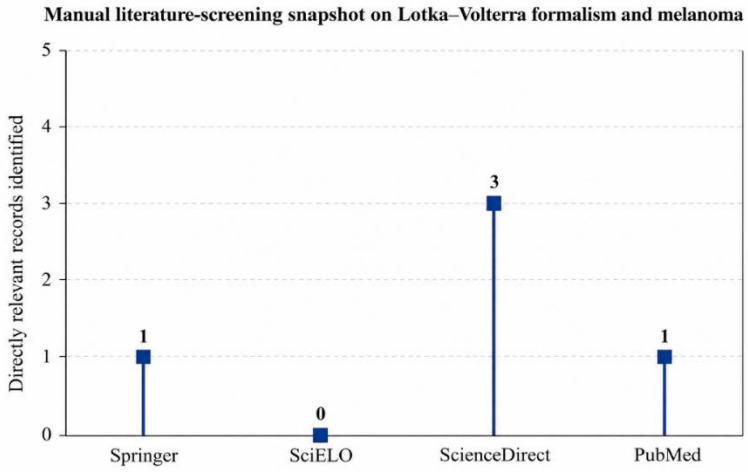

Figure 2: Manual screening snapshot based on keyword combinations such as “Lotka-Volterra” AND melanoma AND (formalism OR derivation OR analytical). The markers represent directly relevant records identified in visible search results, not official database totals. The screening suggests that numerical and applied studies are easier to find than papers centered on explicit formal derivation for melanoma growth.

General Objective

To establish a formal mathematical and computational framework in which the Lotka–Volterra system is derived step by step for melanoma-oriented population dynamics and subsequently coupled to a fractionated radiotherapy input.

Specific Objectives

To derive the Lotka–Volterra system from balance and interaction assumptions; define the biological meaning of its variables and parameters; demonstrate the origin of the bilinear interaction term; analyze the equilibrium, linearization and first-integral structure of the classical system; introduce the radiotherapy dose as an external treatment variable after the analytical derivation; implement the resulting formulation in C++ using fourth-order Runge–Kutta integration; and connect the numerical treatment step to the Geant4 Monte Carlo simulation used for three-dimensional visualization.

Methodology

Table 1. Methodological framework adopted in the present study

Tool / Method	Function in the Study	Application to Melanoma Modeling	Scientific Justification
Formal mathematical derivation	Analytical development of the Lotka–Volterra system	Derivation of the nonlinear interaction equations governing melanoma growth	Provides the theoretical foundation of the mathematical model and establishes the biological interpretation of each equation term.
C++ Programming Language	Computational implementation of the mathematical model	Translation of the Lotka–Volterra equations into executable algorithms	Enables direct incorporation of the mathematical formulation into the Geant4 simulation framework while preserving computational efficiency.
Geant4 Monte Carlo Toolkit	Three-dimensional radiotherapy simulation	Simulation of melanoma regression under a clinically inspired treatment protocol	Accurately models radiation transport and allows dynamic visualization of tumor evolution during treatment.
Medical articles and clinical data	Extraction of clinical treatment parameters	Definition of the radiotherapy protocol and qualitative comparison with reported therapeutic response	Provides biomedical realism and allows the computational results to be interpreted in light of published clinical evidence.
Three-dimensional Geant4 visualization	Generation of scientific images	Visualization of melanoma shrinkage during the five treatment fractions	Facilitates the interpretation of tumor evolution and strengthens the connection between mathematical modeling and clinical application.

Mathematical Formulation, Numerical Implementation and Dose Coupling

The computational methodology is organized in a sequential form. First, the two-population Lotka–Volterra system is constructed analytically from population balances and pairwise interaction assumptions. Second, the resulting ordinary differential equations are solved numerically in C++ using the classical fourth-order Runge–Kutta method. Third, the radiotherapy dose is introduced as an external treatment input acting on the population state between numerical integration intervals. Finally, Geant4 represents the three-dimensional radiation-transport problem and provides the computational dose-deposition component. These stages are deliberately separated so that the analytical model is not confused with the radiation field or with the numerical treatment-response operation.

$\frac{dM}{dt} = aM - bMH \frac{dH}{dt} = -cH + dMH$Let M(t) denote the modeled melanoma-cell population and H(t) the effective growth-limiting host compartment interacting with the melanoma population. Here, H is a phenomenological model variable rather than a claim that a specific host cell type behaves as a biological predator. This definition is adopted explicitly to avoid conflating distinct biological mechanisms. The population model is written as described in the analytical derivation, with a, b, c and d retaining their stated mathematical meanings. The Lotka–Volterra parameters are not redefined as radiation quantities; radiation dose is introduced only after the final analytical system has been obtained.

$X_j^- = \left(M_j^-, H_j^-\right)^T D_j . X_j^+ = \mathrm{R}\left(\mathrm{D_j}, \mathrm{X_j^-}\right) D_j$For treatment fraction j, the population state immediately before irradiation is represented by $X_j^- = \left(M_j^-, H_j^-\right)^T$. The dose associated with that fraction is denoted by D_j. After the numerical ODE evolution, D_j is supplied to the treatment-response operator R, producing $X_j^+ = R\left(D_j, X_j^-\right)$. The post-treatment state is then used as the initial state for the next interval. Thus, the Lotka–Volterra phase space remains two-dimensional, while D_j is an external treatment input.

The C++ implementation presented in this revised manuscript is a new reproducible implementation of the mathematical formulation and is not claimed to be a verbatim recovery of the historical source used in the original simulations. This distinction is intentional: the purpose of the code is to demonstrate that the derived equations can be translated into an executable numerical procedure, while undocumented historical parameter values are not reconstructed or invented.

The Geant4 component represents the three-dimensional irradiation geometry, photon transport and dose deposition. Shen et al. (2025) provide the clinical reference protocol used here: 25 Gy delivered in five fractions of 5 Gy using 6-MV photons. The virtual lesion is treated as a computational geometry and is not a patient-specific reconstruction. Because the historical Geant4 source settings were not retained, this revised manuscript does not invent a physics list, number of particle histories, scoring configuration, or dose uncertainty. These quantities are therefore identified explicitly as reproducibility limitations rather than being presented as undocumented facts.

Mathematical Formulation and Analytical Derivation

Bacaër (2011) documents the independent historical development of mathematically equivalent population-interaction equations by Alfred J. Lotka and Vito Volterra during the 1920s. The original formulation concerned interacting biological populations, while later mathematical oncology studies have adapted related nonlinear population structures to biomedical questions (Aguadé-Gorgorió et al., 2024; Kim et al., 2021; West et al., 2023). In the present article, the formal derivation is the central mathematical contribution: the final Lotka–Volterra equations are obtained from explicit assumptions rather than introduced only as a computational prescription.

In the present article, the Lotka–Volterra system is written in the following melanoma-oriented form:

$$\begin{cases} \dfrac{dM(t)}{dt} = aM(t) - bM(t)H(t), \\ [0.3cm] \dfrac{dH(t)}{dt} = -cH(t) + dM(t)H(t), \end{cases} \tag{1}$$

In the present article, the Lotka–Volterra system is written in the following melanoma-oriented form. M(t) denotes the modeled melanoma-cell population, H(t) denotes the effective growth-limiting host compartment, a is the intrinsic growth rate of melanoma cells, b measures the reduction of melanoma expansion due to interaction, c is the natural depletion rate of H in the absence of melanoma-driven stimulation, and d quantifies the interaction-induced coupling. These definitions are modeling assumptions rather than a claim that H is literally a predator species. The interaction structure is used as a phenomenological mean-field representation of coupled tumor and host effects.

We now derive Eq. (1) step by step. Let M(t) and H(t) be the total sizes of two interacting populations. Over a short time interval [t, t + Δt], the variation in the melanoma population is written as a balance between intrinsic growth and loss caused by interaction:

$$M(t + \Delta t) - M(t) = (\textbf{birth/growth contribution}) - (\textbf{loss due to interaction}). \tag{2}$$

Similarly, for the second population, the variation is written as a gain produced by interaction minus its natural loss:

$$H(t + \Delta t) - H(t) = (\textbf{gain induced by interaction}) - (\textbf{natural loss}). \tag{3}$$

We first construct the intrinsic melanoma-growth term. Assume that, in the absence of interaction, the melanoma population grows proportionally to its current size. Then, over Δt,

$$\Delta M_{\text{free}} = aM(t)\Delta t + o(\Delta t), \tag{4}$$

where $a > 0$ is the intrinsic proliferation rate. Dividing by Δt,

$$\frac{\Delta M_{\text{free}}}{\Delta t} = aM(t) + \frac{o(\Delta t)}{\Delta t}. \tag{5}$$

Taking $\Delta t \to 0$,

$$\lim_{\Delta t \to 0} \frac{\Delta M_{\text{free}}}{\Delta t} = aM(t). \tag{6}$$

To justify the interaction term, we invoke a mass-action assumption. Suppose that the probability of an effective encounter between one melanoma cell and one element of the second population during Δt is proportional to Δt, while the total number of possible encounters is proportional to the product M(t)H(t). Therefore,

$$\Delta N_{\text{enc}} = \kappa M(t)H(t)\Delta t + o(\Delta t), \tag{7}$$

where $\kappa > 0$ is an encounter-rate constant. If each effective interaction removes, on average, a fraction $\eta > 0$ of melanoma cells at the population scale, then

$$\Delta M_{\text{int}} = \eta \Delta N_{\text{enc}} = \eta\kappa M(t)H(t)\Delta t + o(\Delta t). \tag{8}$$

Defining

$$b = \eta\kappa, \tag{9}$$

we obtain

$$\Delta M_{\text{int}} = bM(t)H(t)\Delta t + o(\Delta t). \tag{10}$$

Substituting Eqs. (4) and (10) into Eq. (2),

$$M(t + \Delta t) - M(t) = aM(t)\Delta t - bM(t)H(t)\Delta t + o(\Delta t). \tag{11}$$

Dividing both sides by Δt,

$$\frac{M(t + \Delta t) - M(t)}{\Delta t} = aM(t) - bM(t)H(t) + \frac{o(\Delta t)}{\Delta t}. \tag{12}$$

Taking the limit $\Delta t \to 0$, by the definition of derivative,

$$\frac{dM(t)}{dt} = aM(t) - bM(t)H(t). \tag{13}$$

We now derive the second equation. Assume that, in the absence of melanoma-driven interaction, the second population decays linearly:

$$\Delta H_{\text{free}} = -cH(t)\Delta t + o(\Delta t), \tag{14}$$

with $c > 0$. The interaction, however, produces an induced gain proportional to the same bilinear encounter term:

$$\Delta H_{\text{gain}} = dM(t)H(t)\Delta t + o(\Delta t), \tag{15}$$

where $d > 0$ is the interaction-coupling coefficient. Then Eq. (3) becomes

$$H(t + \Delta t) - H(t) = dM(t)H(t)\Delta t - cH(t)\Delta t + o(\Delta t). \tag{16}$$

Dividing by Δt,

$$\frac{H(t + \Delta t) - H(t)}{\Delta t} = -cH(t) + dM(t)H(t) + \frac{o(\Delta t)}{\Delta t}. \tag{17}$$

Passing to the limit,

$$\frac{dH(t)}{dt} = -cH(t) + dM(t)H(t). \tag{18}$$

Combining Eqs. (13) and (18), we recover exactly the system in Eq. (1). At this point the formal derivation is complete: the classical Lotka–Volterra equations have been obtained from the stated balance laws, intrinsic tendencies, and bilinear interaction assumptions.

For additional formal detail, the bilinear term can also be justified from a density-based integral argument. Let ρ_M and ρ_H be the local densities of the two interacting populations in a spatial region Ω. The total populations are obtained by integrating these densities over Ω. If the local interaction rate per unit volume is proportional to the product ρ_M ρ_H, then integration over the domain yields the total interaction rate. Under a spatially averaged or well-mixed approximation, this rate reduces to a constant multiplied by M(t)H(t), providing the mean-field origin of the nonlinear product.

$$\boldsymbol{M(t) = \int_{\Omega} m\,(\mathrm{x}, t)dV, \qquad H(t) = \int_{\Omega} h\,(\mathrm{x}, t)dV.} \tag{19}$$

Suppose that the local interaction rate per unit volume is proportional to the product of densities:

$$\boldsymbol{q(\mathrm{x}, t) = \lambda m(\mathrm{x}, t)h(\mathrm{x}, t),} \tag{20}$$

with $\lambda > 0$. Then the total interaction rate is

$$\boldsymbol{Q(t) = \int_{\Omega} q\,(\mathrm{x}, t)dV = \lambda \int_{\Omega} m\,(\mathrm{x}, t)h(\mathrm{x}, t)dV.} \tag{21}$$

If one adopts a spatially averaged or well-mixed approximation,

$$\boldsymbol{m(\mathrm{x}, t) \approx \frac{M(t)}{|\Omega|}, \qquad h(\mathrm{x}, t) \approx \frac{H(t)}{|\Omega|},} \tag{22}$$

then

$$\boldsymbol{Q(t) \approx \lambda \int_{\Omega} \frac{M(t)}{|\Omega|}\frac{H(t)}{|\Omega|}dV = \lambda \frac{M(t)H(t)}{|\Omega|^2}\int_{\Omega} dV.} \tag{23}$$

Since

$$\boldsymbol{\int_{\Omega} dV = |\Omega|,} \tag{24}$$

we obtain

$$\boldsymbol{Q(t) \approx \frac{\lambda}{|\Omega|}M(t)H(t).} \tag{25}$$

Defining

$$\boldsymbol{\tilde{\lambda} = \frac{\lambda}{|\Omega|},} \tag{26}$$

it follows that

$$\boldsymbol{Q(t) \approx \tilde{\lambda}M(t)H(t),} \tag{27}$$

which is precisely the origin of the nonlinear interaction product M(t)H(t) under a mean-field approximation. Hence, the bilinear term is not inserted merely for numerical convenience; it follows naturally from the assumption of local pairwise encounters together with spatial averaging.

We may also write the derivation in per-capita form. From Eq. (13),

$$\frac{1}{M}\frac{dM}{dt} = a - bH. \tag{28}$$

Integrating formally over time from 0 to t,

$$\int_0^t \frac{1}{M(s)}\frac{dM(s)}{ds}\,ds = \int_0^t \big(a - bH(s)\big)\,ds. \tag{29}$$

Applying the chain rule in reverse on the left-hand side,

$$\int_0^t \frac{d}{ds}\ln M(s)\,ds = at - b\int_0^t H(s)\,ds. \tag{30}$$

By the fundamental theorem of calculus,

$$\ln M(t) - \ln M(0) = at - b\int_0^t H(s)\,ds. \tag{31}$$

Therefore,

$$M(t) = M(0)\exp\left(at - b\int_0^t H(s)\,ds\right). \tag{32}$$

Similarly, from Eq. (18),

$$\frac{1}{H}\frac{dH}{dt} = -c + dM, \tag{33}$$

and integration gives

$$H(t) = H(0)\exp\left(-ct + d\int_0^t M(s)\,ds\right). \tag{34}$$

These identities show explicitly that each population evolves according to its own intrinsic tendency corrected by the accumulated interaction with the other population. The derivation therefore establishes the mathematical structure before any radiotherapy variable is introduced.

We now compute the equilibrium points by setting both time derivatives equal to zero.

$$\frac{dM}{dt} = 0, \qquad \frac{dH}{dt} = 0, \tag{35}$$

the system becomes

$$aM - bMH = 0, \qquad -cH + dMH = 0. \tag{36}$$

Factorizing,

$$M(a - bH) = 0, \qquad H(-c + dM) = 0. \tag{37}$$

Hence either

$$M = 0 \quad \text{or} \quad H = \frac{a}{b}, \tag{38}$$

and either

$$H = 0 \quad \text{or} \quad M = \frac{c}{d}. \tag{39}$$

Thus the equilibrium points are

$$E_0 = (0,0), \qquad E_* = \left(\frac{c}{d}, \frac{a}{b}\right). \tag{40}$$

The nontrivial equilibrium is especially relevant because it defines the characteristic balance point between melanoma proliferation and interaction-mediated limitation.

For local linear analysis, define

$$f(M,H) = aM - bMH, \qquad g(M,H) = -cH + dMH. \tag{41}$$

The Jacobian matrix is

$$J(M,H) = \begin{pmatrix} \frac{\partial f}{\partial M} & \frac{\partial f}{\partial H}[0.3cm] \frac{\partial g}{\partial M} & \frac{\partial g}{\partial H} \end{pmatrix} = (a - bH \quad -bM[0.2cm] dH \quad -c + dM). \tag{42}$$

Evaluating at $E_* = \left(\frac{c}{d}, \frac{a}{b}\right)$,

$$J(E_*) = \left(a - b\left(\frac{a}{b}\right) \quad -b\left(\frac{c}{d}\right)[0.3cm] d\left(\frac{a}{b}\right) \quad -c + d\left(\frac{c}{d}\right)\right) = \left(0 \quad -\frac{bc}{d}[0.3cm] \frac{ad}{b} \quad 0\right). \tag{43}$$

The characteristic polynomial is

$$\det(J(E_*) - \lambda I) = det\begin{pmatrix} -\lambda & -\frac{bc}{d}[0.3cm] \frac{ad}{b} & -\lambda \end{pmatrix} = \lambda^2 + ac. \tag{44}$$

Hence

$$\lambda = \pm i\sqrt{ac}. \tag{45}$$

This classical result explains the center-type oscillatory structure of the Lotka–Volterra interaction near the coexistence equilibrium. It is important for interpretation because the unmodified classical system is conservative rather than an attracting tumor-regression model.

A useful first integral of the system may also be derived. Dividing the equations eliminates time and produces a separable relation between M and H:

$$\frac{dH}{dM} = \frac{\frac{dH}{dt}}{\frac{dM}{dt}} = \frac{H(-c + dM)}{M(a - bH)}. \tag{46}$$

Rearranging,

$$\frac{a - bH}{H} dH = \frac{-c + dM}{M} dM. \tag{47}$$

Expanding both sides,

$$\left(\frac{a}{H} - b\right) dH = \left(-\frac{c}{M} + d\right) dM. \tag{48}$$

Integrating,

$$\int \left(\frac{a}{H} - b\right) dH = \int \left(-\frac{c}{M} + d\right) dM. \tag{49}$$

Thus the resulting quantity is constant along trajectories. This first-integral structure is consistent with the closed-orbit behavior of the classical Lotka–Volterra system.

$$a\int \frac{1}{H} dH - b\int dH = -c\int \frac{1}{M} dM + d\int dM, \tag{50}$$

Shen et al. (2025) report a stage-IV melanoma case with a defined radiotherapy prescription, including total dose, fractionation and photon energy. These clinical quantities are used here as a reference treatment protocol for the computational experiment, not as a direct patient-specific calibration of the Lotka–Volterra parameters.

$$a\ln H - bH = -c\ln M + dM + C. \tag{51}$$

The reference protocol consists of 25 Gy delivered in five fractions of 5 Gy each using 6-MV photons (Shen et al., 2025). The numerical model therefore receives the fraction-specific dose D_j after the analytical Lotka–Volterra equations have already been derived. This ordering is important: dose is an external treatment input and is not inserted into the classical two-population equations as a third state variable.

$$dM - c\ln M + bH - a\ln H = C, \tag{52}$$

Numerical Implementation in C++ and Radiotherapy Dose Coupling

The dose-coupling law used in the revised numerical implementation is a phenomenological treatment-response operator. The coefficient α controls the fractional reduction of the modeled melanoma population produced by the dose D_j delivered in treatment fraction j. The operator is deliberately separated from the Lotka–Volterra coefficients a, b, c and d. It is not presented as a replacement for the linear-quadratic radiobiological model; rather, it is the compact dose-response rule used to demonstrate how an external radiotherapy input updates the population state.

$$M_j^+ = M_j^- \, exp(-\alpha D_j) \tag{53}$$

For the present computational demonstration, α is fixed at 0.20 Gy^{-1}. This value is adopted as a reproducible model parameter and is not claimed to be a patient-specific calibration. Published radiobiological studies show substantial heterogeneity in α and β estimates, so quantitative clinical use would require calibration to an appropriate melanoma dataset (van Leeuwen et al., 2018).

Dose-to-volume mapping

To make the connection between the modeled melanoma population and the three-dimensional lesion explicit, the present formulation assumes a constant effective cellular density. Under this normalization, the modeled population M is proportional to the computational tumor volume V. If V_0 and M_0 denote the initial computational volume and initial modeled melanoma population, respectively, the pre- and post-fraction volumes are written as:

$$V_j^- = V_0(M_j^-/M_0), \quad V_j^+ = V_0(M_j^+/M_0) = V_j^- \, exp(-\alpha D_j) \tag{54}$$

For the three-dimensional visualization, the lesion is represented by an ellipsoidal geometry. When R is the base radius and Z is the full ellipsoidal height, its geometric volume is:

$$V = (4\pi/3)\, R^2(Z/2) = (2\pi/3)\, R^2 Z \tag{55}$$

Equations (54)–(55) provide the requested mathematical bridge from dose to the modeled tumor state and from the modeled state to the three-dimensional geometric representation. Because V_0 and the population-to-volume proportionality are not independently calibrated against patient measurements in the present study, the per-fraction geometric values in Table 6 remain computational descriptors rather than independently predicted clinical tumor volumes.

The computational sequence is therefore: analytical Lotka–Volterra model → RK4 numerical integration → fraction-specific dose → treatment-response update → dose-to-volume mapping → next Lotka–Volterra interval. This preserves the two-dimensional mathematical meaning of the population model while making the radiation component explicit.D_j

```
#include <cmath>
#include <iomanip>
#include <iostream>
#include <vector>

struct State {
   double M;  // normalized melanoma population
   double H;  // normalized interacting population
};

State rhs(const State& x, double a, double b, double c, double d) {
   return {
      a * x.M - b * x.M * x.H,
      -c * x.H + d * x.M * x.H
   };
}

State rk4_step(const State& x, double dt,
            double a, double b, double c, double d) {
   const State k1 = rhs(x, a, b, c, d);

   const State x2{x.M + 0.5 * dt * k1.M,
               x.H + 0.5 * dt * k1.H};
   const State k2 = rhs(x2, a, b, c, d);

   const State x3{x.M + 0.5 * dt * k2.M,
               x.H + 0.5 * dt * k2.H};
   const State k3 = rhs(x3, a, b, c, d);

   const State x4{x.M + dt * k3.M,
               x.H + dt * k3.H};
   const State k4 = rhs(x4, a, b, c, d);

   return {
      x.M + (dt / 6.0) * (k1.M + 2.0*k2.M + 2.0*k3.M + k4.M),
      x.H + (dt / 6.0) * (k1.H + 2.0*k2.H + 2.0*k3.H + k4.H)
   };
}

void apply_dose(State& x, double D, double alpha) {
   x.M *= std::exp(-alpha * D);
}

double volume_from_population(double V0, double M, double M0) {
   return V0 * (M / M0);
}

int main() {
   // Fixed numerical parameters reported in Table 2.
   const double a = 1.0;      // day^-1
   const double b = 1.0;      // day^-1, normalized populations
   const double c = 1.0;      // day^-1
   const double d = 1.0;      // day^-1, normalized populations
   const double alpha = 0.20;  // Gy^-1
   const double M0 = 1.0;
   const double H0 = 1.0;
```

```
    const double dt = 0.01;     // day
    const double V0 = 1.0;      // normalized initial computational volume

    const std::vector<double> dose = {5.0, 5.0, 5.0, 5.0, 5.0}; // Gy
    State x{M0, H0};

    std::cout << std::fixed << std::setprecision(6);

    for (std::size_t j = 0; j < dose.size(); ++j) {
       // One treatment interval is represented here by one day.
       for (double t = 0.0; t < 1.0; t += dt) {
          x = rk4_step(x, dt, a, b, c, d);
       }

       const State before = x;
       const double Vbefore = volume_from_population(V0, before.M, M0);

       apply_dose(x, dose[j], alpha);

       const double Vafter = volume_from_population(V0, x.M, M0);

       std::cout << "Fraction " << (j + 1)
                 << " | D = " << dose[j] << " Gy"
                 << " | M- = " << before.M
                 << " | M+ = " << x.M
                 << " | V- / V0 = " << Vbefore
                 << " | V+ / V0 = " << Vafter
                 << " | H+ = " << x.H << '\n';
    }

    return 0;
}
```

The code above is intentionally compact but self-contained and executable. It defines the Lotka–Volterra right-hand side, performs fourth-order Runge–Kutta integration with the reported numerical parameters, applies the fraction-specific dose through the explicit treatment-response coefficient α, and also evaluates the normalized dose-to-volume mapping defined in Eqs. (54)–(55). The source is a new reproducible implementation of the revised mathematical formulation and is not claimed to recover the historical source code.

For the Monte Carlo execution, the reported configuration used the following Geant4 event call, with N = 100000 primary histories:

runManager->BeamOn(100000);

This call specifies the number of primary events used for the reported Monte Carlo calculation.

Table 4. Symbols and their roles in the mathematical and computational model.

Symbol	Meaning in the model	Role in computation
M(t)	Modeled melanoma population	State variable updated by the ODE and treatment step
H(t)	Second interacting population / growth-limiting compartment	State variable of the Lotka–Volterra system
a	Intrinsic melanoma growth rate	Coefficient in dM/dt
b	Interaction coefficient reducing M	Coefficient of −bMH
c	Natural depletion rate of H	Coefficient in dH/dt
d	Interaction-induced coupling coefficient	Coefficient of +dMH
D_j	Dose associated with fraction j	External treatment input; not a Lotka–Volterra state variable
R	Treatment-response operator	Maps pre-fraction state and dose to post-fraction state

Equation (1) is therefore the mathematical core of the study. Its importance lies in the fact that the model is not introduced as a black-box numerical formula: the nonlinear interaction term is derived from explicit population assumptions, the final

system is analyzed mathematically, and only then is the equation translated into C++. The radiation dose is subsequently introduced as an external treatment input, creating a transparent bridge between analytical modeling, numerical integration, and the Geant4 radiotherapy simulation.

Computational Parameter and Reproducibility Statement

The revised implementation is parameter-explicit and uses a fixed numerical set for the present computational demonstration. The melanoma and host variables M(t) and H(t) are treated as normalized, dimensionless population variables, so a, b, c and d all have units of day^{-1} in the present formulation. The adopted values are $a = b = c = d = 1.0$ day^{-1}, $M_0 = H_0 = 1.0$, $\Delta t = 0.01$ day, and $\alpha = 0.20$ Gy^{-1}. These values are stated explicitly to make the numerical procedure reproducible. They are model parameters for the computational demonstration and are not presented as patient-specific fitted quantities. The choice of α is consistent with the order of magnitude of α values summarized in radiobiological modeling, but the substantial heterogeneity of published estimates means that clinical prediction would require independent calibration (van Leeuwen et al., 2018).

Parameter	Meaning	Dimension	Value used in present study
a	Intrinsic melanoma growth rate	day^{-1}	1.0 day^{-1}
b	Melanoma–H interaction coefficient	day^{-1} (normalized M,H)	1.0 day^{-1}
c	Natural depletion rate of H	day^{-1}	1.0 day^{-1}
d	Interaction-induced coupling coefficient	day^{-1} (normalized M,H)	1.0 day^{-1}
M_0	Initial modeled melanoma population	dimensionless	1.0
H_0	Initial H population	dimensionless	1.0
Δt	Numerical integration step	day	0.01 day
α	External dose-response coefficient	Gy^{-1}	0.20 Gy^{-1}

Table 2. Numerical parameter set used in the present C++ implementation. The values are explicitly adopted for reproducible computation and are not claimed as patient-specific calibration.

Parameter-selection note. The values $a = b = c = d = 1.0$ day^{-1}, $M_0 = H_0 = 1.0$ and $\Delta t = 0.01$ day are adopted to produce a transparent, normalized and reproducible numerical demonstration. The dose-response coefficient $\alpha = 0.20$ Gy^{-1} is likewise adopted for the present model; it lies within the order of magnitude of α values summarized in the radiobiological literature, but it is not a melanoma-specific clinical fit (van Leeuwen et al., 2018).

For the Geant4 component (Agostinelli et al., 2003), the retained computational configuration includes a Varian TrueBeam reference with 6-MV photon irradiation, a 10 × 10 cm^2 field, a broad-beam configuration, normal incidence on the skin-surface geometry, field collimation, and an ellipsoidal virtual lesion. The primary particle is a photon (gamma), and beam fluence is represented in particles per unit area. Source-to-surface and source-to-axis distances were defined as part of the treatment geometry, although their numerical values are not preserved in the retained record. The retained computational notes identify G4EmStandardPhysics and Penelope as the electromagnetic treatment used; because the historical constructor configuration is no longer available, the manuscript does not assert a more specific constructor combination than the retained record supports. The simulation used 10^5 (100,000) primary histories, with deposited energy scored using G4PSEnergyDeposit, and the reported relative dose uncertainty was 2.4%. These settings are now stated explicitly to improve reproducibility without inventing undocumented values.

Geant4 item	Information in revised manuscript	Status
Beam / energy	Varian TrueBeam; 6-MV photon beam; primary photons treated as monoenergetic in the computational setup	Reported
Field	10 × 10 cm^2; broad-beam configuration; collimated field	Reported
Beam direction	Normal/perpendicular incidence to the skin-surface geometry	Reported
Source geometry	Source position; SSD/SAD defined by treatment geometry; numerical distances not retained	Partially reported
3D geometry	Ellipsoidal virtual melanoma lesion on a skin-surface geometry	Reported
Particle type	Photon (gamma)	Reported
Fluence / intensity	Particles per unit area	Reported
Physics treatment	G4EmStandardPhysics and Penelope, as identified in the retained computational notes; exact constructor configuration not preserved	Reported with configuration limitation
Particle histories	10^5 primary histories (100,000 events)	Reported
Scoring configuration	G4PSEnergyDeposit; deposited energy scoring	Reported
Dose uncertainty	Relative uncertainty: 2.4%	Reported

Total / fractionation	25 Gy; 5 × 5 Gy	Reported
Dose deposition	Geant4 Monte Carlo radiation transport and energy-deposition scoring	Reported

Table 3. Geant4 beam, geometry, scoring and reproducibility information available from the retained computational record.

Results and Discussion

The computational experiment uses the published melanoma radiotherapy protocol as a clinically inspired reference (Shen et al., 2025). The protocol specifies 25 Gy delivered in five fractions of 5 Gy using 6-MV photons. The numerical implementation uses a = b = c = d = 1.0 day^{-1}, $M_0 = H_0 = 1.0$, $\Delta t = 0.01$ day, and $\alpha = 0.20$ Gy^{-1}, as specified in Table 2. The fraction-specific dose is applied after each numerical integration interval, so radiation remains an external treatment input rather than a third Lotka–Volterra population.$M_j^+ = M_j^- \exp(-\alpha D_j)$

The derived Lotka–Volterra system was translated into C++ using fourth-order Runge–Kutta integration and coupled to the Geant4 Monte Carlo workflow. Between fractions, the population state evolves according to the ordinary differential equations; at each fraction, the corresponding 5-Gy dose is applied through the external treatment response. The same update is mapped to normalized tumor volume through Eq. (54). The Geant4 configuration used a 10 × 10 cm² broad photon field, normal incidence, an ellipsoidal virtual lesion, 10^5 primary histories, G4PSEnergyDeposit scoring, and a reported relative dose uncertainty of 2.4%.

Table 5 summarizes the clinical reference parameters and their computational representation. Table 6 reports the available per-fraction geometric estimates used to describe the progressive reduction shown in Figures 3–7. These estimates are reported separately from the dose-response law: the law updates the modeled melanoma state, whereas the three-dimensional lesion geometry provides the visual and geometric representation.

Table 5. Clinical reference parameters and their corresponding computational representation

Clinical Parameter	Reported Clinical Data	Simulation Model (Geant4)
Disease	Stage IV malignant melanoma of unknown primary (MUP)	Virtual melanoma lesion
Patient	60-year-old male	Clinically inspired computational model
Radiotherapy target	Superficial abdominal melanoma lesion	Three-dimensional skin-surface lesion
Selected radiotherapy protocol	Abdomen 1	Reproduced in simulation
Total prescribed dose	25 Gy	25 Gy
Fractionation	5 fractions	5 simulated fractions
Dose per fraction	5 Gy	5 Gy
Irradiation technique	SBRT	Monte Carlo radiotherapy simulation
Linear accelerator	Varian TrueBeam	Clinical irradiation conditions reproduced
Photon energy	6 MV photons	6 MV photon beam
Treatment frequency	One fraction per day (Monday–Friday)	Same clinical schedule considered
Initial lesion volume	281.53 cm³	Reference geometry value; not independently predicted by the uncalibrated model
Final lesion volume	48.00 cm³	Reference-case value; no independent quantitative model prediction claimed
Reference volumetric reduction	82.95%	Reference-case value; not attributed to calibrated Lotka–Volterra prediction
Mathematical model	—	Lotka–Volterra equations implemented in C++
Computational platform	—	Geant4 Monte Carlo Toolkit
Simulation output	Clinical treatment response	Three-dimensional melanoma regression throughout five fractions

Table 6. Per-fraction geometric descriptors and estimated lesion volumes available from the retained computational record

Fraction	Relative height (ΔZ)	Base radius (R)	Estimated volume
Fraction 1	1.00 mm (reference)	~ 2.5 mm (reference)	48
Fraction 2	~ 0.85 mm	~ 2.1 mm	~ 28–30
Fraction 3	~ 0.60 mm	~ 1.7 mm	~ 13–15
Fraction 4	~ 0.30 mm	~ 1.2 mm	~ 3–5
Fraction 5	~ 0.05 mm	~ 0.5 mm	~ 0.1–0.5

Note. The numerical volume estimates are reproduced on the computational scale retained in the source record. The retained source image does not preserve a sufficiently reliable unit label for these per-fraction estimates; therefore, no unit is assigned to them here. The independent clinical reference values of 281.53 cm^3 initially and 48.00 cm^3 finally are retained in Table 5 and are not equated numerically to the per-fraction geometric estimates.

Interpretation of Figure 3

The first fraction represents the initial stage of the computational treatment scenario. After delivery of 5 Gy, the lesion retains most of its initial spatial extent. The retained geometric descriptors are approximately 1.00 mm in relative height and 2.5 mm in base radius, with an estimated volume of 48 on the computational scale reported in Table 6. The image establishes the reference three-dimensional state against which the subsequent fractions are compared.

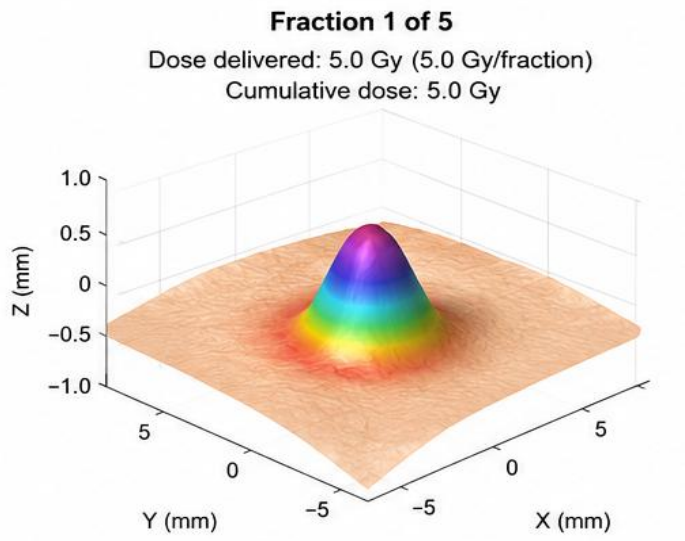

Figure 3. Three-dimensional simulation of melanoma during Fraction 1 of the clinical radiotherapy protocol. A dose of 5 Gy was delivered, corresponding to a cumulative dose of 5 Gy.

Interpretation of Figure 4

After the second 5-Gy fraction, the cumulative dose reaches 10 Gy. The retained geometry decreases to approximately 0.85 mm in relative height and 2.1 mm in base radius, corresponding to an estimated volume of approximately 28–30 on the retained computational scale. The reduction is consistent with the progressive contraction represented in the three-dimensional visualization.

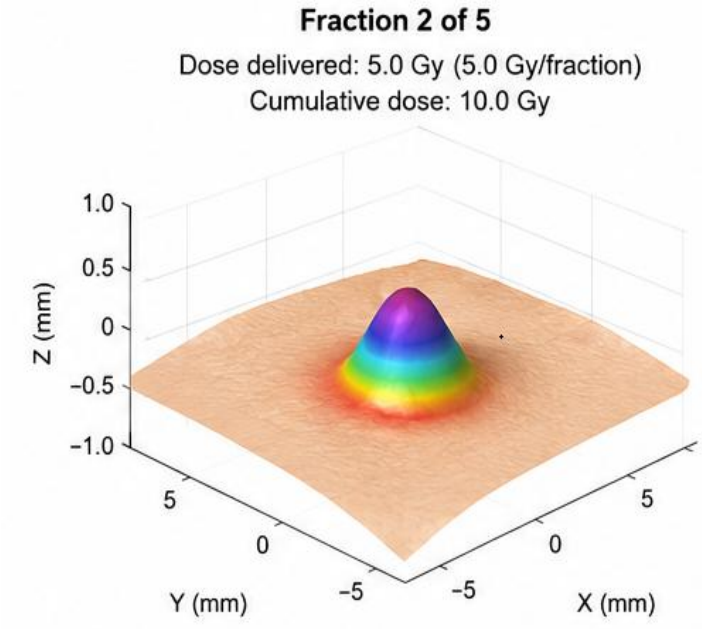

Figure 4. Three-dimensional simulation of melanoma during Fraction 2 of the clinical radiotherapy protocol. A second dose of 5 Gy increases the cumulative delivered dose to 10 Gy, producing an initial reduction in the simulated tumor volume.

Interpretation of Figure 5

At the midpoint of the treatment schedule, the cumulative dose reaches 15 Gy. The relative height is approximately 0.60 mm and the base radius approximately 1.7 mm, with an estimated volume of approximately 13–15 on the retained computational scale. The figure therefore shows the continued geometric reduction as additional treatment fractions are applied.

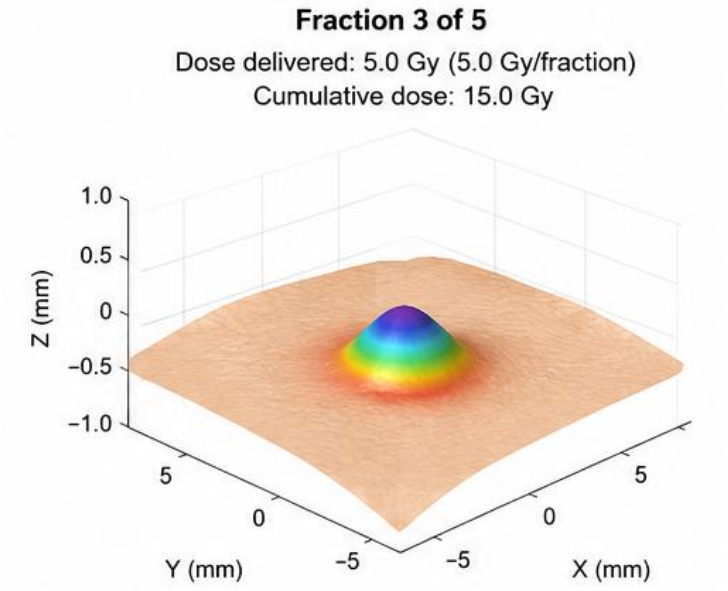

Figure 5. Three-dimensional simulation of melanoma during Fraction 3 of the clinical radiotherapy protocol. The cumulative dose reaches 15 Gy, producing a more pronounced reduction in the modeled lesion.

Interpretation of Figure 6

Following the fourth fraction, the cumulative dose reaches 20 Gy. The retained geometry is approximately 0.30 mm in relative height and 1.2 mm in base radius, with an estimated volume of approximately 3–5 on the retained computational scale. The result illustrates the marked reduction in the modeled lesion before completion of the prescribed course.

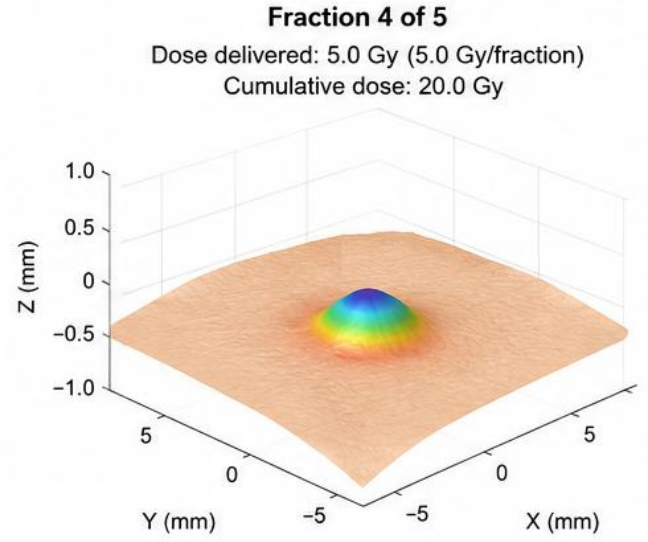

Figure 6. Three-dimensional simulation of melanoma during Fraction 4 of the clinical radiotherapy protocol. After delivery of 20 Gy, the lesion becomes considerably smaller while maintaining its spatial localization on the skin surface.

Interpretation of Figure 7

The fifth fraction completes the prescribed 25-Gy course. The retained geometry reaches approximately 0.05 mm in relative height and 0.5 mm in base radius, with an estimated volume of approximately 0.1–0.5 on the retained computational scale. This final image summarizes the treatment scenario represented by the coupled workflow. As stated throughout the manuscript, these geometric estimates describe the computational visualization and are not claimed as an independently calibrated patient-specific tumor-volume prediction.

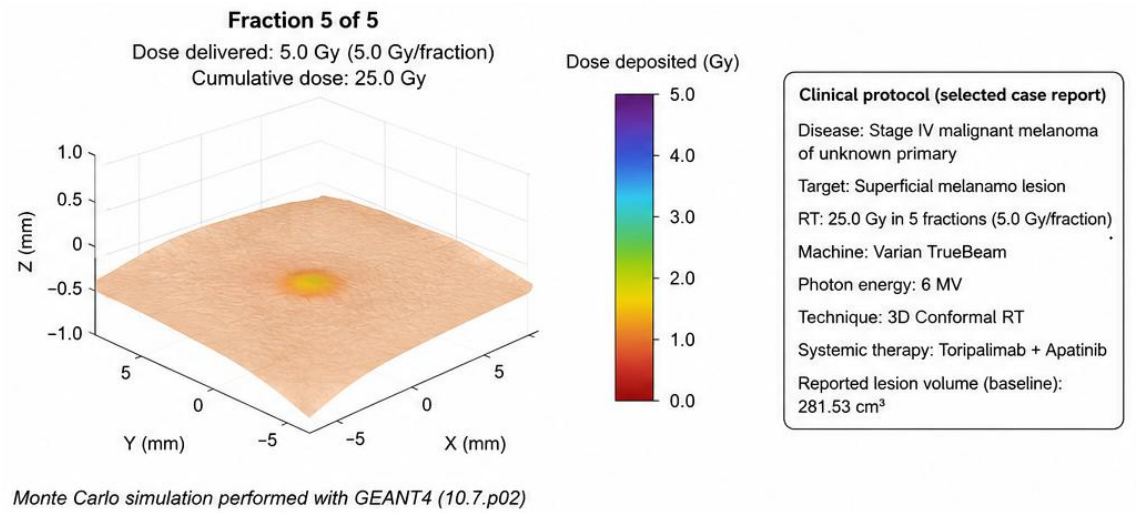

Figure 7. Final three-dimensional simulation of melanoma after Fraction 5 of the clinical radiotherapy protocol. The complete prescribed dose of 25 Gy has been delivered, resulting in the minimum simulated tumor volume observed throughout the treatment.

Taken together, Figures 3–7 show a progressive visual reduction of the modeled lesion throughout the five-fraction treatment scenario, from a cumulative dose of 5 Gy to 25 Gy. The sequence does not introduce a third population into the Lotka–Volterra system; instead, radiation dose is treated as an external treatment input applied between numerical integration intervals. This distinction preserves the two-dimensional mathematical structure of the Lotka–Volterra phase space while allowing the computational workflow to represent fractionated radiotherapy.

The results should therefore be understood as a computational demonstration of the coupling between formal mathematical derivation, numerical integration, external dose input, and three-dimensional Monte Carlo radiation transport. The available clinical protocol provides the irradiation schedule and reference geometry, whereas the three-dimensional images visualize the treatment scenario. No independent patient-specific validation or quantitative dose-to-volume calibration is claimed.

Conclusion

This work presented a formal and computational framework for investigating melanoma growth and radiotherapy response using the Lotka–Volterra system. The principal contribution is the explicit analytical derivation of the nonlinear population equations from balance laws, intrinsic growth or depletion assumptions, and bilinear interaction principles. The resulting equations are then translated into a numerical C++ implementation, rather than being used only as a black-box computational model.

D_jA central feature of the formulation is the separation between the mathematical population model and the radiation treatment variable. The symbols a, b, c and d retain their biological meanings in the Lotka–Volterra equations, while the dose for fraction j is represented separately by D_j. The dose is introduced only after the final analytical system has been obtained, through an explicit treatment-response operator. Consequently, radiation dose is not interpreted as a third Lotka–Volterra population.

The C++ implementation provides a reproducible numerical realization of the analytical model using fourth-order Runge–Kutta integration and an explicitly stated dose-response step. Geant4 supplies the three-dimensional radiation-transport and dose-deposition environment. The resulting images therefore represent a clinically inspired computational demonstration of the treatment workflow rather than an independently validated patient-specific prediction.

The mathematical analysis also establishes an important limitation of the untreated classical system. Its nontrivial equilibrium has purely imaginary linearized eigenvalues and a conservative first-integral structure, corresponding to closed trajectories rather than an attracting limit cycle. Therefore, irreversible tumor regression should not be attributed to the unmodified Lotka–Volterra equations; it enters through the external treatment coupling introduced after the analytical derivation.

The C++ implementation provides a reproducible numerical realization of the analytical model using fourth-order Runge–Kutta integration and an explicitly stated dose-response step. Geant4 supplies the three-dimensional radiation-transport and dose-deposition environment. The numerical values used for a, b, c, d, M_0, H_0, Δt and α are now reported explicitly; however, they should be interpreted as computationally adopted parameters rather than patient-specific fitted quantities. Independent calibration remains necessary before any quantitative clinical prediction is attempted.

Despite these limitations, the framework establishes a transparent sequence from mathematical derivation to numerical solution, external dose coupling, and three-dimensional radiotherapy visualization. The study therefore emphasizes formal mathematical modeling as a complement to computational simulation and clearly separates demonstrated results from quantities that require future calibration or independent validation.

References

1. Agostinelli, S., Allison, J., Amako, K., Apostolakis, J., Araujo, H., Arce, P., Asai, M., Axen, D., Banerjee, S., Barrand, G., Behner, B., Bellagamba, G., Boudreau, J., Broglia, L., Brunengo, A., Burkhardt, H., Chauvie, S., Chuma, J., Chytracek, R., Cosmo, G., Depaola, G., Dietrich, D., Enami, R., Feliciello, A., Ferguson, C., Fesefeldt, H., Folger, G., Forti, A., Garelli, S., Giani, S., Giannitrapani, R., Gibin, D., Greeniaus, G., Greiner, W., Grossheim, A., Guatelli, S., Gumplinger, P., Hamatsu, R., Hashimoto, H., Hasui, K., Heikkinen, A., Howard, A., Huh, J., Kadi, Y., Kanaya, N., Kawabata, F., Kawabata, M., Kawabata, Y., Kossov, V., Kurashige, H., Lamanna, E., Lara, V., Lattanzi, R., Lechner, A., Lee, F., Legrá, J., Lessard, L., Li, W., Lockman, W., Longo, F., Maire, M., Mancini-Terracciano, A., Mantero, A., Masai, M., McCormick, J., McLaren, I., Mendez, A., Menéndez, A., Meridiani, P., Minamimoto, K., Murakami, K., Musumarra, A., Nagamatsu, K., Nash, R., Nieminen, P., Nikitina, T., Nowak, L., Pandola, L., Paprocki, P., Parlati, S., Peralta, L., Perl, J., Pfeiffer, A., Pia, M. G., Ranjard, F., Rybin, A., Sadilov, S., Salvo, E. D., Sasaki, T., Sawada, H., Scherer, S., Sei, S., Sirotenko, V., Smith, M., Starkov, N., Stepanenko, A., Tanaka, S., Tcherniaev, E., Tomaradze, A., Truscott, P., Uno, H., Urban, L., Verderi, M., Wenaus, T., Williams, D., Wright, D., Yamada, T., Yoshida, H., & Zschiesche, D. (2003). Geant4—a simulation toolkit. Nuclear Instruments and Methods in Physics Research Section A: Accelerators, Spectrometers, Detectors and Associated Equipment, 506(3), 250–303. https://doi.org/10.1016/S0168-9002(03)01368-8
2. Aguadé-Gorgorió, G., Anderson, A. R. A., & Solé, R. (2024). Modeling tumors as complex ecosystems. iScience, 27, 110699. https://doi.org/10.1016/j.isci.2024.110699
3. Altrock, P. M., Liu, L. L., & Michor, F. (2015). The mathematics of cancer: Integrating quantitative models. Nature Reviews Cancer, 15, 730–745. https://doi.org/10.1038/nrc4029
4. Bacaër, N. (2011). Lotka, Volterra and the predator–prey system (1920–1926). In A short history of mathematical population dynamics. Springer. https://doi.org/10.1007/978-0-85729-115-8_13
5. Beerenwinkel, N., Schwarz, R. F., Gerstung, M., & Markowetz, F. (2015). Cancer evolution: Mathematical models and computational inference. Systematic Biology, 64(1), e1–e25. https://doi.org/10.1093/sysbio/syu081
6. Bruningk, S. C., Mikell, E. K., & Scott, J. A. (2023). Mathematical modeling of radiotherapy: Impact of model selection on estimating minimum radiation dose for tumor control. Frontiers in Oncology, 13, 1130966. https://doi.org/10.3389/fonc.2023.1130966
7. Gallasch, R., Efremova, M., Charoentong, P., Hackl, H., & Trajanoski, Z. (2013). Mathematical models for translational and clinical oncology. Journal of Clinical Bioinformatics, 3, 23. https://doi.org/10.1186/2043-9113-3-23
8. Huang, J., Chan, S. C., Ko, S., Lok, V., Zhang, L., Lin, X., Lucero-Prisno III, D. E., Xu, W., Zheng, Z.-J., Elcarte, E., Withers, M., & Wong, M. C. S. (2023). Global incidence, mortality, risk factors and trends of melanoma: A systematic analysis of registries. American Journal of Clinical Dermatology, 24, 965–975. https://doi.org/10.1007/s40257-023-00795-3
9. Kim, E., Brown, J. S., Eroglu, Z., & Anderson, A. R. A. (2021). Adaptive therapy for metastatic melanoma: Predictions from patient calibrated mathematical models. Cancers, 13(4), 823. https://doi.org/10.3390/cancers13040823
10. Shen, J., Ge, Y., Zhang, P., Gao, H., & Wang, L. (2025). Diverse radiotherapy fractionation in malignant melanoma: A case report. Frontiers in Oncology, 15, 1662686. https://doi.org/10.3389/fonc.2025.1662686
11. Siegel, R. L., Kratzer, T. B., Giaquinto, A. N., Sung, H., & Jemal, A. (2025). Cancer statistics, 2025. CA: A Cancer Journal for Clinicians. https://doi.org/10.3322/caac.21871
12. van Leeuwen, C. M., Oei, A. L., Crezee, J., Bel, A., Franken, N. A. P., Stalpers, L. J. A., & Kok, H. P. (2018). The alfa and beta of tumours: A review of parameters of the linear-quadratic model, derived from clinical radiotherapy studies. Radiation Oncology, 13, 96. https://doi.org/10.1186/s13014-018-1040-z
13. West, J. R., Mareschal, J., Jarrett, A. M., & Anderson, A. R. A. (2023). Computational approaches to modelling and optimizing cancer treatment. Nature Reviews Bioengineering, 1. https://doi.org/10.1038/s44222-023-00089-7